Unoccupied electronic structure of $Y_{1-x}Ca_xTiO_3$ investigated by inverse photoemission spectroscopy

M. Arita,[1] H. Sato,[1] M. Higashi,[2] K. Yoshikawa,[2] K. Shimada,[1] M. Nakatake,[1] Y. Ueda,[2] H. Namatame,[1] M. Taniguchi,[1,2]
M. Tsubota,[3] F. Iga,[3] and T. Takabatake[3]

[1]*Hiroshima Synchrotron Radiation Center, Hiroshima University, 2-313 Kagamiyama, Higashi-Hiroshima 739-0046, Japan*
[2]*Graduate School of Science, Hiroshima University, 1-3-1 Kagamiyama, Higashi-Hiroshima 739-8530, Japan*
[3]*Graduate School of Advanced Sciences of Matter, Hiroshima University, 1-3-1 Kagamiyama, Higashi-Hiroshima 739-8530, Japan*
(Received 16 December 2006; published 24 May 2007)

We have studied the unoccupied electronic structure of the band insulator $CaTiO_3$, the Mott insulator $YTiO_3$, and $Y_{0.61}Ca_{0.39}TiO_3$ with a metal-insulator transition (MIT) around 150 K by means of Ti $3p$-$3d$ resonant inverse photoemission spectroscopy (RIPES). The Ti $3d$ partial density of states of $CaTiO_3$ deduced from the on- and off-resonance RIPES spectra is in good agreement with results of a band-structure calculation, while that of $YTiO_3$ is explained based on a calculation with the dynamical mean-field theory taking into account an electron correlation. In the case of $Y_{0.61}Ca_{0.39}TiO_3$, we have successfully observed the temperature dependence of RIPES spectra across MIT; the intensity of the incoherent part (a remnant of the upper Hubbard bands) relative to the coherent part (quasiparticle bands) is reduced with decreasing temperature from the insulator to metal phases.

PACS number(s): 71.27.+a, 71.30.+h, 79.60.−i

I. INTRODUCTION

The $3d$ transition-metal (TM) oxides with a perovskite-type structure have attracted much interest because of their unusual electronic and magnetic properties which originate from strong electron correlation, such as a colossal negative magnetoresistance.[1] Among them, it is well known that carrier doping to the TM $3d$ bands and control of the $3d$ bandwidth give rise to a metal-insulator transition (MIT). According to the Mott-Hubbard picture, MIT is caused by a change in the relative magnitude between the on-site $3d$-$3d$ Coulomb interaction U_{d-d} and $3d$ bandwidth W (U_{d-d}/W). If the number of the $3d$ electrons for one Ti site is an integer, an energy splitting between the lower and upper Hubbard bands increases with increasing U_{d-d}/W, and MIT takes place at $U_{d-d}/W \sim 1$.

There has been a considerable amount of work on occupied electronic states of the perovskite TM oxides investigated by means of photoemission spectroscopy (PES).[1–12] According to the results, as a system in the metal phase approaches the insulator phase, the spectral weight transfers from quasiparticle bands near the Fermi level (E_F) (that is, the coherent part) to a remnant of the lower Hubbard bands (that is, the incoherent part). For these Mott-Hubbard systems, the dynamical mean-field theory (DMFT) has been applied to explain the PES and optical spectra.[12–16] The PES spectra of $SrVO_3$ and $CaVO_3$, categorized into the typical Mott-Hubbard system, are well reproduced by band-structure calculations with the local-density approximation (LDA) taking into account electron correlation using DMFT. On the other hand, there has been only little experimental information on unoccupied electronic structure of the Mott-Hubbard systems, so far.[6,7,17] Since DMFT gives electronic structure for conduction bands as well as valence bands, information on the unoccupied parts is crucial to understand the physical properties of the Mott-Hubbard systems.

$Y_{1-x}CA_xTiO_3$ with a distorted perovskite structure ($GdFeO_3$ type) is a system varying from the d^1 insulator $YTiO_3$ ($x=0$) to d^0 insulator $CaTiO_3$ ($x=1$). The system is metallic for the Ca composition x from $\sim$0.4 to $\sim$0.9. $YTiO_3$ is well known as the d^1 Mott insulator with a ferromagnetism below the Curie temperature of $T_c=30$ K, while $CaTiO_3$ is classified as a d^0 band insulator. The physical properties and electronic structures of $Y_{1-x}Ca_xTiO_3$ have been studied using polycrystals.[18,19] PES and inverse photoemission spectroscopy (IPES) experiments have been performed for polycrystals, and the spectral changes occurring on Ca doping have been reported.[7]

Single-crystal $Y_{0.61}Ca_{0.39}TiO_3$ is an insulator at room temperature and exhibits a clearer temperature-induced MIT around 150 K than when polycrystalline. With decreasing temperature, the electrical resistivity along the c axis decreases from $\sim$1 to $\sim 10^{-3}$ Ω cm steeply at MIT temperature. Hysteresis of the resistivity suggests a strong coupling between electronic states and lattice distortion.[20,21] Previously, we have measured temperature-dependent PES spectra of $Y_{0.61}Ca_{0.39}TiO_3$ single crystals. MIT is clearly observed as the spectral weight transfers from the incoherent to coherent parts with decreasing temperature.[22,23]

In this paper, we report the unoccupied overall and Ti $3d$ electronic structure of single-crystal $CaTiO_3$, $YTiO_3$, and $Y_{0.61}Ca_{0.39}TiO_3$ investigated by means of IPES with bremsstrahlung-isochromat-spectroscopy (BIS) mode (BIS-IPES) and Ti $3p$-$3d$ resonant IPES (RIPES) with tunable-photon-energy mode.

The experimental results of $CaTiO_3$ and $YTiO_3$ are discussed based on the band-structure calculation and that using DMFT, respectively. It is shown that the MIT of $Y_{0.61}Ca_{0.39}TiO_3$ is observed in the temperature-dependent Ti $3d$ partial density of states (DOS) deduced from the RIPES spectra.

II. EXPERIMENTS

$Y_{1-x}Ca_xTiO_3$ single crystals were grown by a floating-zone method.[20,21] The grown samples were characterized by
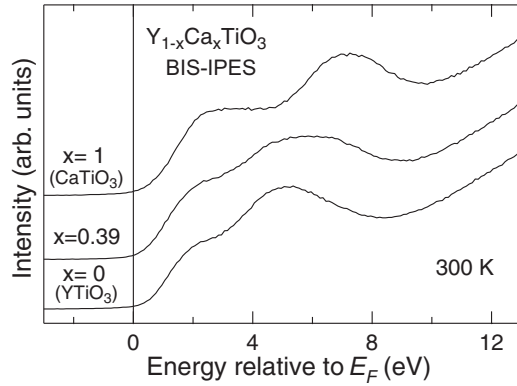
FIG. 1. BIS-IPES spectra of $CaTiO_3$, $YTiO_3$, and $Y_{0.61}Ca_{0.39}TiO_3$ measured at 300 K. Emitted photon energy of $h\nu = 9.4$ eV is detected.

their Laue images, powder x-ray diffraction, and electron-probe microanalysis. As for $Y_{0.61}Ca_{0.39}TiO_3$, MIT was found to take place at around 150 K in the electrical resistivity measurement.

BIS-IPES measurements were done at 300 and 110 K using an IPES spectrometer equipped with an Erdman-Zipt-type low-energy electron gun using a BaO cathode and a bandpass-type photon detector centered at $h\nu = 9.4$ eV.[24,25] The incidence angle of the electrons was normal to the sample surface. The total energy resolution was 0.56 eV and the working pressure of the analysis chamber was 1×10^{-10} Torr. The temperature of the samples was maintained with a liquid N_2 refrigerator.

The Ti $3p$-$3d$ RIPES spectra were measured using the same type of electron gun as used in BIS-IPES. Emitted photons from the samples were monochromatized by a varied line-spacing spherical grating with averaged line density of 1200 lines/mm and detected using a CsI-coated multichannel plate.[26] The total energy resolution was estimated to be 0.55 eV at $E_k = 46$ eV, where E_k denotes the kinetic energy of the incident electrons, and working pressure of the analysis chamber was 3×10^{-10} Torr. The angle between the axes of the e-gun and the monochromator was 45° and the incidence angle of the electrons was set to about 20° from the surface normal. The temperature of samples was controlled between 17 and 300 K by a combination of the closed-cycle He refrigerator and heater. For BIS-IPES and RIPES measurements, E_F was determined from the Fermi edge of the spectra for a fresh Au film, and clean surfaces were obtained by fracturing *in situ*.

III. RESULTS AND DISCUSSION

Figure 1 shows the BIS-IPES spectra of $CaTiO_3$, $YTiO_3$, and $Y_{0.61}Ca_{0.39}TiO_3$ measured at 300 K. The abscissa represents energy above E_F. The spectra have been normalized using the intensity around 12 eV. All spectra exhibit two structures near E_F and between 4 and 10 eV. The energy position of the structure between 4 and 10 eV depends on the compounds, and shifts from ~7.3 eV for $CaTiO_3$ to ~5 eV for $YTiO_3$. In the spectrum of $Y_{0.61}Ca_{0.39}TiO_3$, the structure
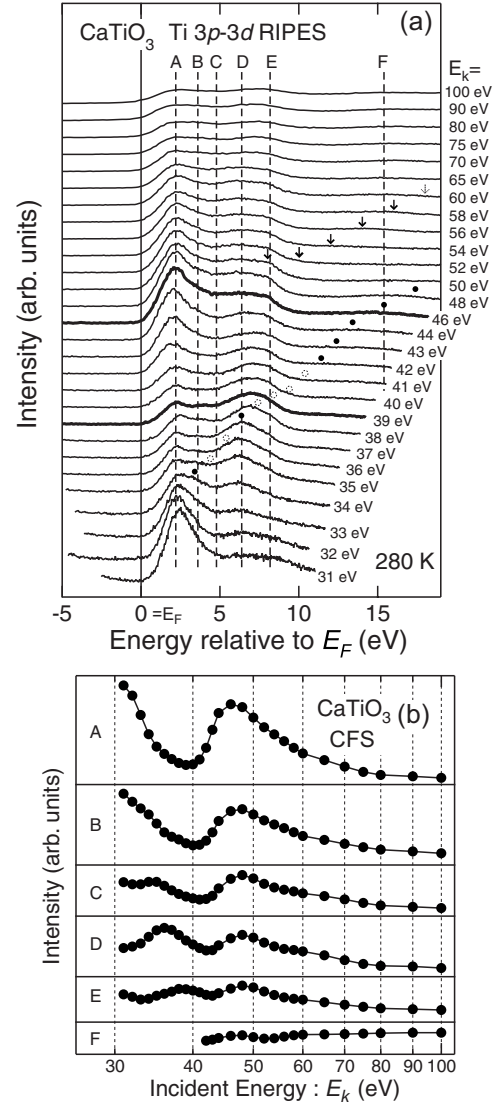
FIG. 2. (a) E_k dependence of RIPES spectra of $CaTiO_3$ measured at 280 K including the Ti $3p$-$3d$ absorption region. Structures indicated by dots and arrows are the Ca $3d \rightarrow 3p$ and Ti $3d \rightarrow 3p$ fluorescence peaks, respectively. (b) CFS spectra of $CaTiO_3$ for the structures labeled A–F in (a). In the spectrum of A, intensity exhibits the maximum and minimum at $E_k = 46$ and 39 eV, corresponding to the Ti $3p$-$3d$ on- and off-resonances, respectively.

around 6 eV is assumed to be composed of the two components from structures of $CaTiO_3$ and $YTiO_3$, and attributed to the unoccupied Ca $3d$ and Y $4d$ states. On the other hand, the spectral feature near E_F does not change appreciably for compounds, and these structures are ascribed to the unoccupied Ti $3d$ states. We have found almost no temperature dependence in the BIS-IPES spectrum of $Y_{0.61}Ca_{0.39}TiO_3$ between 300 and 110 K across MIT.

Figure 2(a) displays the E_k dependence of RIPES spectra of $CaTiO_3$ measured at 280 K. The spectra have been normalized using the intensity around 10.5 eV.[27] In the figure, vertical broken lines specify energy positions of (A) 2.2, (B) 3.6, (C) 4.8, (D) 6.4, (E) 8.2, and (F) 15.4 eV. It should be noticed that the spectral feature depends significantly on E_k, in particular, from 31 to 50 eV including the Ti $3p$-$3d$ ab-

sorption region. The RIPES spectrum at $E_k=31$ eV shows two structures around (A) 2.2 and (D) 6.4 eV. With increasing E_k, 6.4 eV peak D is enhanced at $E_k=36$ eV, while 2.2 eV peak A reaches maximum at $E_k=46$ eV. Two broad structures indicated by dots and arrows move toward the higher-energy side with E_k. These structures are observed at constant emission photon energies of $h\nu \sim 34$ and ~ 44.7 eV, indicating that these structures are due to the Ca $3d \rightarrow 3p$ and Ti $3d \rightarrow 3p$ fluorescence peaks, respectively.[28]

To see the E_k dependence of the spectra in detail, we trace the intensity of the structures specified by labels A–F as a function of E_k in Fig. 2(b). The derived curves correspond to constant final-state (CFS) spectra. The CFS spectrum for A shows the largest amount of intensity change with a maximum at $E_k=46$ eV and a minimum at 39 eV. In comparison with the constant initial-state (CIS) spectra of Ti$_2$O$_3$ (Ref. 29) in the Ti $3p$-$3d$ resonant PES, and CFS spectra of Nb-doped SrTiO$_3$ (Refs. 17 and 30) in the Ti $3p$-$3d$ resonant PES and RIPES, this behavior is interpreted on the basis of the Ti $3p$-$3d$ resonant inverse photoemission process.

The Ti $3d$ normal IPES process is expressed by

$$|3p^6 3d^n\rangle + e^- \rightarrow |3p^6 3d^{n+1}\rangle + h\nu, \qquad (1)$$

where e^- and $h\nu$ represent an incident electron and an emitted photon, respectively. n is the configuration number of the $3d$ electrons and $n=0$ for CaTiO$_3$. On the other hand, in the Ti $3p$-$3d$ absorption region, the following RIPES process accompanied by the super Coster-Kronig decay takes place:

$$|3p^6 3d^n\rangle + e^- \rightarrow |3p^5 3d^{n+2}\rangle \rightarrow |3p^6 3d^{n+1}\rangle + h\nu. \qquad (2)$$

Since the initial and final states are the same for the two processes (1) and (2), they interfere with each other. Thus, the cross section of the Ti $3d$ states changes remarkably with E_k in the Ti $3p$-$3d$ absorption region.

In the CFS spectrum for A, the intensity change due to the interference effect is clearly recognized, indicating that the Ti $3d$ states dominantly contribute to this energy region of 2.2 eV. From the maximum and minimum intensities of the spectrum, $E_k=46$ and 39 eV can be regarded as the Ti $3p$-$3d$ on- and off-resonance energies, respectively. Intensities of the CFS spectra for B–E have their maxima at $E_k=48$ eV, higher by ~ 2 eV than that at $E_k=46$ eV for A and the extent of their enhancement is weaker than that of A.

The Ti $3d$ bands split into t_{2g} and e_g orbitals due to the octahedral crystal field. The e_g orbitals extend toward the apical oxygen ion and strongly hybridized with the O $2p$ orbitals, forming the broad bands. On the other hand, the Ti $3d$ t_{2g}-O $2p$ hybridization is weak and the t_{2g} bands are narrow in comparison with the e_g bands. The structures A and B–E are, thus, attributed to the unoccupied t_{2g} and e_g bands, respectively, judging from a difference in the amount of the intensity change between the structures A and B–E.

The CFS spectra for C, D, and E exhibit peaks also between $E_k=33$ and 39 eV. Since these peaks are not observed in the CFS spectrum for 6 eV structure in TiO$_2$ (not shown), they are not related to the Ti- or O-derived states. From the CIS spectra of Ca metal with strong resonance and a minimum at $h\nu=25$ eV and a maximum at $h\nu=33$ eV,[31] the peaks between $E_k=33$ and 39 eV are derived from the
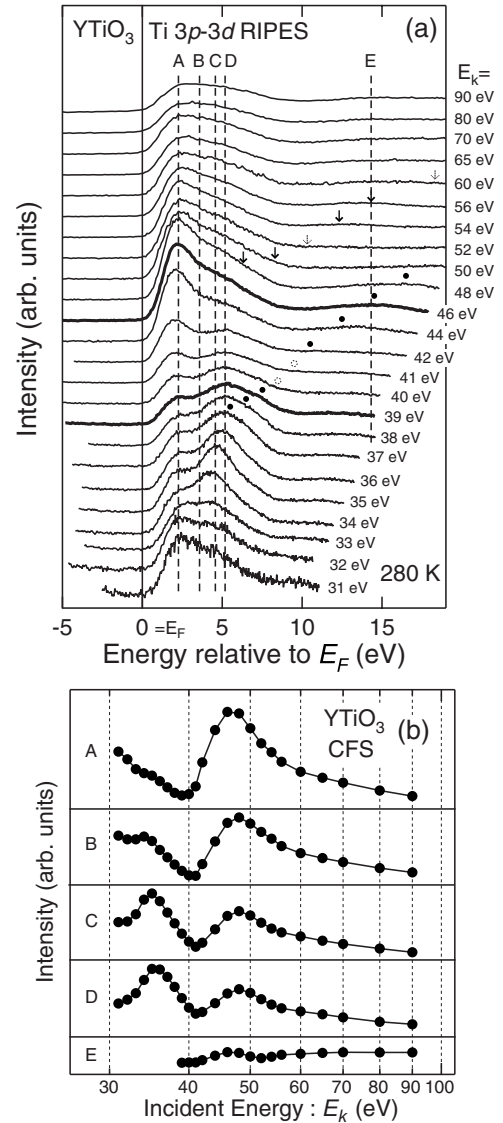
FIG. 3. (a) E_k dependence of RIPES spectra of YTiO$_3$ measured at 280 K including the Ti $3p$-$3d$ absorption region. The structures indicated by dots and arrows are the Y $4d \rightarrow 4p$ and Ti $3d \rightarrow 3p$ fluorescence peaks, respectively. (b) CFS spectra of YTiO$_3$ for the structures labeled A–F in (a). In the spectrum of A, the intensity exhibits the maximum and minimum at $E_k=46$ and 39 eV, corresponding to the Ti $3p$-$3d$ on- and off-resonances, respectively.

Ca $3p$-$3d$ resonance, and the structures C–E in Fig. 2(a) are attributed to the Ca $3d$ states. The largest enhancement of D indicates that the Ca $3d$ states contribute dominantly to the energy region around D, which is clearly observed also in the BIS-IPES spectrum in Fig. 1. Since the CFS spectrum for F exhibits no resonance, the structure F is due to the Ti $4sp$ states. Two small humps at $E_k \sim 46$ and ~ 58 eV arise from overlaps of the Ca $3d \rightarrow 3p$ and Ti $3d \rightarrow 3p$ fluorescence peaks, respectively.

Figure 3(a) shows E_k dependence of RIPES spectra of YTiO$_3$ measured at 280 K. We find that two structures around (A) 2.2 and (C) 4.8 eV are mainly enhanced at $E_k=39$ and 46 eV, respectively. The two broad structures indicated by dots and arrows are the Y $4d \rightarrow 4p$ and Ti $3d$
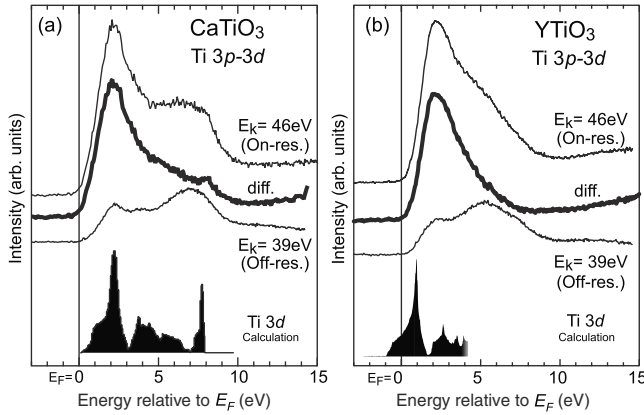
FIG. 4. On- and off-resonance RIPES spectra (thin lines) and the difference spectra (thick lines) of (a) CaTiO₃ and (b) YTiO₃ in comparison with the theoretical partial DOS's of Ti 3d states (Refs. 32 and 34).

$\rightarrow 3p$ fluorescence peaks. The CFS spectra for the structures at (A) 2.2, (B) 3.8, (C) 4.8, (D) 5.2, and (E) 14.3 eV are presented in Fig. 3(b). The enhancement of structure A around $E_k = 46$ eV is attributed to the Ti 3p-3d resonance as the spectra of CaTiO₃, and the structures B–D around $E_k = 37$ eV, stem from the Y 4p-4d resonance. Using the same line of argument for CaTiO₃, structures A, B–D, and E are attributed to the Ti $3d$ t_{2g}, Y $4d$ together with the Ti $3d$ e_g, and Ti $4sp$ states, respectively.

Unoccupied Ti 3d partial DOS's of CaTiO₃ and YTiO₃ have been deduced by subtracting off-resonance spectrum from the on-resonance spectrum. These results are shown in the upper parts of Figs. 4(a) and 4(b) as difference spectra (thick lines) together with the on- and off-resonance spectra (thin lines). One notices that the difference spectra have no intensity at E_F and that the Ti 3d states contribute dominantly to ~2.2 eV for both compounds. In addition, the off-resonance spectra for both compounds are similar to the BIS-IPES spectra in Fig. 1 with respect to the two structures near E_F and between 4 and 10 eV, because of the small cross section of the Ti 3d states for the BIS-IPES spectra measured with $h\nu = 9.4$ eV.

Here we compare the difference spectra with the theoretical Ti 3d partial DOS's of CaTiO₃ and YTiO₃ in the lower parts of Figs. 4(a) and 4(b), respectively. The theoretical Ti 3d partial DOS of CaTiO₃ in Fig. 4(a) is calculated by means of the tight-binding linear muffin-tin orbital method within the atomic sphere approximation for a cubic perovskite-type structure,[32] assuming that E_F is located at conduction-band minimum. The narrow structure below 3 eV is derived from the Ti $3d$ t_{2g} states, and the broad structure between 3 and 8 eV is due to the Ti $3d$ e_g states hybridized with the O 2p and Ca 3d states. It should be noticed that the difference spectrum of CaTiO₃ is in fairly good agreement with the theoretical DOS including the bandwidth. The structures around 3.7 eV, which are buried by the strong tail from the main peak around 2.2 eV toward the higher-energy side in the difference spectrum, are also clearly observed in the off-resonance spectrum. These results show that CaTiO₃ is a typical band insulator, well explained in terms of the one-electron band theory.[33]
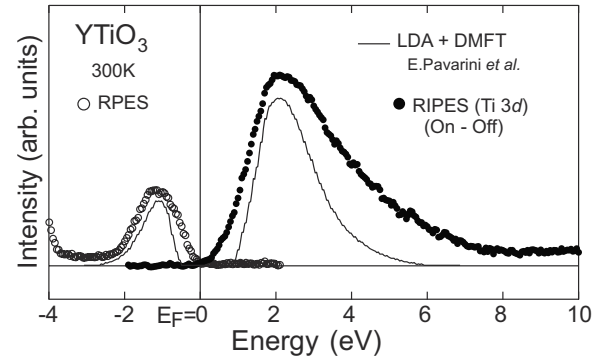
FIG. 5. Comparison of the experimental Ti 3d partial DOS deduced from resonant PES (open circles) and RIPES (closed circles) with the calculated DMFT-DOS (line) (Ref. 36).

The theoretical Ti 3d partial DOS of YTiO₃ in Fig. 4(b), derived from the band-structure calculation with LDA for a paramagnetic phase,[34] is similar to that of CaTiO₃ with respect to the spectral features below 4 eV. E_F exists at 1 eV above the bottom of the Ti 3d bands, reflecting that the Ti 3d bands are partially occupied. The calculated DOS is metallic and the Ti $3d$ t_{2g} bands contribute to the energy region around 1 eV. On the other hand, the experimental difference spectrum shows no intensity at E_F in spite of the $3d^1$ system and the main peak shows up around 2.2 eV, higher than the theoretical DOS by ~1 eV. These discrepancies between the experiments and band-structure calculations are not contradictory to the fact that YTiO₃ is regarded as a Mott insulator with strong electron correlation.

Figure 5 shows a comparison of the experimental Ti 3d spectra of YTiO₃, with the results of DMFT taking into account the electron correlation. Closed circles represent the difference spectrum between the on- and off-resonance RIPES spectra and open circles the Ti 3p-3d resonant PES spectrum taken at $h\nu = 46$ eV, which almost reflects the occupied Ti 3d partial DOS.[35] The correction due to the electron correlation, to the Ti $3d$ t_{2g} partial DOS derived from the LDA calculation with the GdFeO₃-type lattice distortion, is made using DMFT and the modified t_{2g} DOS's are shown as line spectra for the valence and conduction-band regions (DMFT-DOS).[36]

It should be noted that the experimental results are reproduced by the DMFT-DOS with respect to the feature of asymmetric single peaks for both occupied and unoccupied states and their energy separation of ~3.3 eV. Since the single peaks in the occupied and unoccupied parts are attributed to the lower and upper Hubbard bands, respectively, the effective U_{d-d} is, thus, experimentally derived to be ~3.3 eV. We find, however, some discrepancies in the tail toward the higher-energy side of the difference spectrum in the unoccupied part and the amount of the energy gap. The difference in the tail is due to the fact that the DMFT-DOS is calculated only for the Ti $3d$ t_{2g} states excluding the Ti $3d$ e_g states. The amount of energy gap in the experimental spectra is not reproduced by DMFT-DOS, even if the energy resolution of the experiments and thermal broadening effect are considered. Further theoretical studies are apparently required.

Next, we move to results and discussion of the temperature-dependent RIPES of Y₀.₆₁Ca₀.₃₉TiO₃ with MIT.
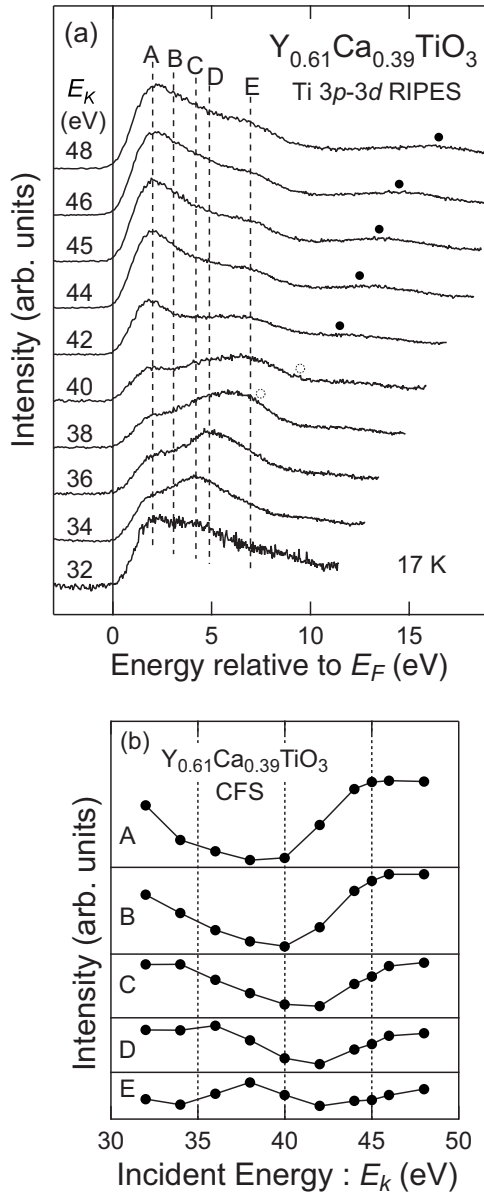
FIG. 6. (a) E_k dependence of RIPES spectra for Y$_{0.61}$Ca$_{0.39}$TiO$_3$ measured at 17 K around the Ti $3p$-$3d$ absorption region. The structures indicated by dots are the Ti $3d\rightarrow3p$ fluorescence peaks. (b) CFS spectra for the structures labeled A–F in (a). In the spectrum of A, the intensity exhibits the maximum and minimum at E_k=46 and 38 eV, corresponding to the Ti $3p$-$3d$ on- and off-resonances, respectively.

Figure 6(a) shows E_k dependence of the spectra measured at 17 K. These spectra have been normalized using the intensity around 10.5 eV.[27] The spectral features are quite similar to those of CaTiO$_3$ and YTiO$_3$. The structures indicated by dots are due to the Ti $3d\rightarrow3p$ fluorescence. The CFS spectra for A–E specified in Fig. 6(a) are shown in Fig. 6(b). One can recognize that the spectra are similar to those of CaTiO$_3$ and YTiO$_3$. Structure A is due to the Ti $3d\ t_{2g}$ states and B–E to the Ti $3d\ e_g$ states. Weak enhancements around E_k =36 eV for D and E are derived from the Ca $3d$ and/or Y $4d$ components.

In order to reveal the change of the Ti $3d$ states in Y$_{0.61}$Ca$_{0.39}$TiO$_3$ across MIT, we have measured the tempera-
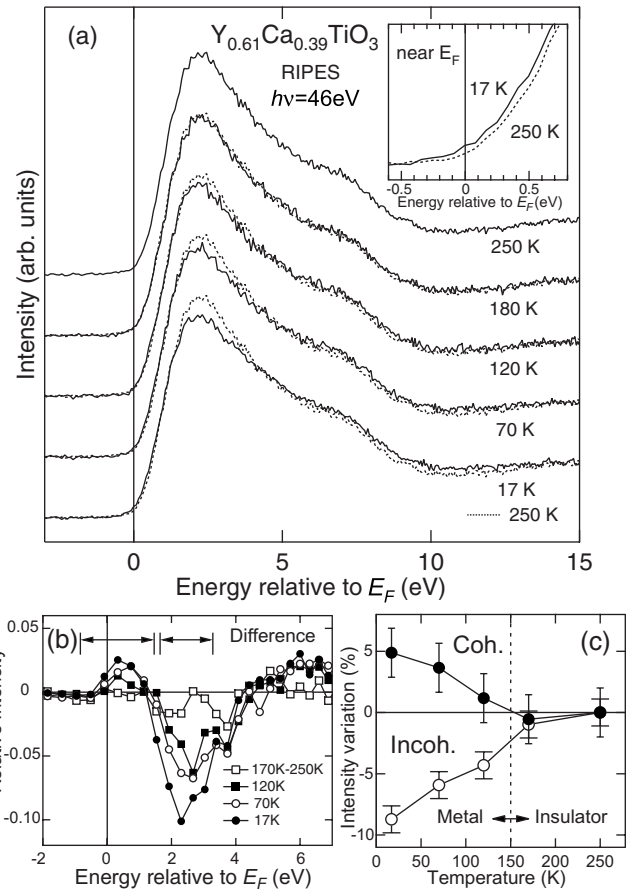
FIG. 7. (a) On-resonance RIPES spectra of Y$_{0.61}$Ca$_{0.39}$TiO$_3$ measured at 17, 70, 120, 180, and 250 K. The spectrum at 250 K is presented by broken lines on each spectrum for comparison. Spectra near E_F are shown in the inset. (b) Difference spectra obtained by subtracting the spectrum at 250 K from that at respective temperatures. (c) Variation of the integrated intensities in the difference spectra for each part of $\sim E_F$ and $\sim$2.2 eV (coherent and incoherent parts, respectively) as a function of temperature. The integrated ranges are indicated by horizontal arrows in (b).

ture dependence of the on-resonance RIPES spectra at E_k=46 eV. Figure 7(a) shows the on-resonance spectra measured at 17, 70, 120, 180, and 250 K. The spectra have been normalized using the intensity integrated between -3 and 17 eV. The spectrum at 250 K is presented by a broken line on each spectrum for comparison. The intensity of the peak around 2.2 eV is reduced with decreasing temperature. In addition, we find a slight change near E_F between 250 and 17 K as shown in the inset. To make clear the behavior of these temperature dependences, we subtract the spectrum at 250 K from the spectra at the respective temperatures in Fig. 7(b). The ordinate is the intensity relative to the maximum intensity of the RIPES spectrum at 250 K around 2.2 eV. It should be noted that the spectral weight of the difference spectra near E_F is positive; that is, the spectral weight increases with decreasing temperature, reflecting the temperature-induced metallic behavior. Alternatively, the structure around 2.2 eV decreases in intensity with decreasing temperature.

Figure 7(c) shows the variations of the intensities integrated near E_F and around 2.2 eV in the difference spectra.
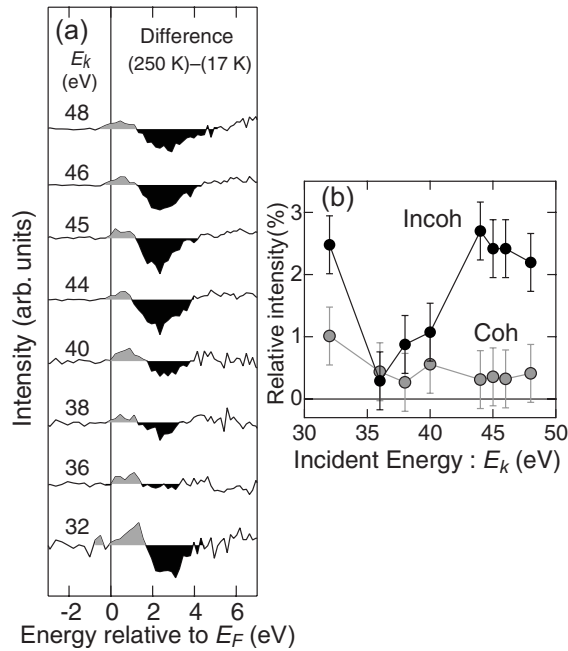
FIG. 8. (a) E_k dependence of difference spectra of $Y_{0.61}Ca_{0.39}TiO_3$ between 17 and 250 K. In all the spectra, the coherent part (gray) is positive and the incoherent part (black) is negative. (b) Integrated intensities of the coherent (gray) and incoherent (black) parts as a function of E_k.

The integrated ranges are indicated by horizontal arrows in Fig. 7(b). The variations are relative to the intensity of the RIPES spectrum at 250 K integrated for each range; that is, the ordinate represents the ratio of the intensities of the difference spectra to that of the RIPES spectrum at 250 K integrated in each energy range. With decreasing temperature, both intensities near E_F and around 2.2 eV start to change below the MIT temperature of 150 K (Ref. 21) and the spectral weight transfers from the region around 2.2 eV to the region near E_F. We find in Figs. 7(b) and 7(c) that the temperature dependence of the RIPES spectra is symmetrical to that of the PES spectra with respect to E_F; the spectral weight in the PES spectrum transfers from the region around 1.4 eV to the region near E_F.[23] Accordingly, we can reasonably assume that the 2.2 eV peak corresponds to the incoherent part (that is, a remnant of the upper Hubbard bands), while the structure near E_F corresponds to the coherent part (that is, the quasiparticle bands). Although the energy position of the incoherent part relative to E_F ($\sim$2.2 eV) in the RIPES spectra is higher than that of PES ($\sim$−1.4 eV), MIT is observed as the spectral weight transfers from the incoherent to coherent parts for both occupied and unoccupied states.

Figure 8(a) shows the E_k dependence of difference spectra between 17 and 250 K, which are derived from the RIPES spectra normalized using the intensity integrated between −3 and 11 eV, and Fig. 8(b) shows the integrated intensities of the coherent (gray) and incoherent (black) parts relative to the intensity of RIPES spectra integrated between −3 and

11 eV. In all the spectra in Fig. 8(a), one sees positive and negative intensities in the coherent and incoherent parts, respectively. In addition, the integrated intensity of the incoherent part exhibits remarkable E_k dependence and reaches a maximum at E_k=44 eV, close to the Ti 3p-3d on-resonance energy, and a minimum (nearly zero) at E_k=36 eV, close to the Ti 3p-3d off-resonance energy. The intensity of the coherent part is, on the other hand, almost unchanged for E_k in contrast to the incoherent part and, in particular, exhibits no remarkable enhancement around E_k=46 eV. These results reveal that the incoherent part mainly consists of the localized Ti 3d states due to large $U_{d\text{-}d}/W$, while the coherent part stems from the delocalized Ti 3d bands hybridized with the other conduction electronic states such as O 2p states. The spectral weight transfer from the incoherent to coherent parts with decreasing temperature implies that the localized Ti 3d states hybridize with the conduction-band states, mainly O 2p states, below the MIT temperature.

As mentioned above, the BIS-IPES spectra with the small cross section of the Ti 3d states exhibit no temperature-dependent features between 280 and 110 K. The off-resonance RIPES spectra at E_k=36 eV also show no remarkable temperature-dependent features. These results indicate that the change of the electronic structure of $Y_{0.61}Ca_{0.39}TiO_3$ across MIT takes place mainly in the Ti 3d states.

IV. CONCLUSION

We have studied the unoccupied electronic structure of the band insulator $CaTiO_3$, the Mott insulator $YTiO_3$, and $Y_{0.61}Ca_{0.39}TiO_3$ with MIT by means of BIS-IPES and RIPES. The unoccupied Ti 3d partial DOS's of these compounds have been deduced from the on- and off-resonance spectra. The Ti 3d DOS feature of $CaTiO_3$ is well reproduced with the band-structure calculation,[32] while overall features of $YTiO_3$ are in good agreement with the Ti 3d t_{2g} DOS calculated with DMFT taking into account the electron correlation. These results reveal that $CaTiO_3$ is a typical band insulator and $YTiO_3$ can be regarded as a Mott insulator, where the whole Ti 3d t_{2g} bands are modified by $U_{d\text{-}d}$.

For $Y_{0.61}Ca_{0.39}TiO_3$, the RIPES spectral weight transfers from the region of $\sim$2.2 eV to the region near E_F with decreasing temperature across MIT. From the temperature dependence of the spectra, we conclude that the coherent and incoherent parts exist near E_F and around 2.2 eV, respectively. In addition, from the E_k dependences of intensity change of the incoherent and coherent parts between 17 and 250 K, the incoherent part is derived from the localized Ti 3d states and the coherent part from the delocalized Ti 3d states hybridized mainly with the O 2p states below the MIT temperature.

[1] M. Imada, A. Fujimori, and Y. Tokura, Rev. Mod. Phys. **70**, 1039 (1998).

[2] A. Fujimori, I. Hase, H. Namatame, Y. Fujishima, Y. Tokura, H. Eisaki, S. Uchida, K. Takegahara, and F. M. F. de Groot, Phys. Rev. Lett. **69**, 1796 (1992).

[3] A. Fujimori, I. Hase, M. Nakamura, H. Namatame, Y. Fujishima, Y. Tokura, M. Abbate, F. M. F. de Groot, M. T. Czyzyk, J. C. Fuggle, O. Strebel, F. Lopez, M. Domke, and G. Kaindl, Phys. Rev. B **46**, 9841 (1992).

[4] Y. Aiura, F. Iga, Y. Nishihara, H. Ohnuki, and H. Kato, Phys. Rev. B **47**, 6732 (1993).

[5] I. H. Inoue, I. Hase, Y. Aiura, A. Fujimori, Y. Haruyama, T. Maruyama, and Y. Nishihara, Phys. Rev. Lett. **74**, 2539 (1995).

[6] K. Morikawa, T. Mizokawa, K. Kobayashi, A. Fujimori, H. Eisaki, S. Uchida, F. Iga, and Y. Nishihara, Phys. Rev. B **52**, 13711 (1995).

[7] K. Morikawa, T. Mizokawa, A. Fujimori, Y. Taguchi, and Y. Tokura, Phys. Rev. B **54**, 8446 (1996).

[8] T. Higuchi, T. Tsukamoto, N. Sata, M. Ishigame, Y. Tezuka, and S. Shin, Phys. Rev. B **57**, 6978 (1998).

[9] I. H. Inoue, O. Goto, H. Makino, N. E. Hussey, and M. Ishikawa, Phys. Rev. B **58**, 4372 (1998).

[10] K. Maiti, P. Mahadevan, and D. D. Sarma, Phys. Rev. Lett. **80**, 2885 (1998).

[11] T. Yoshida, A. Ino, T. Mizokawa, A. Fujimori, Y. Taguchi, T. Katsufuji, and Y. Tokura, Europhys. Lett. **59**, 258 (2002).

[12] A. Sekiyama, H. Fujiwara, S. Imada, S. Suga, H. Eisaki, S. I. Uchida, K. Takegahara, H. Harima, Y. Saitoh, I. A. Nekrasov, G. Keller, D. E. Kondakov, A. V. Kozhevnikov, T. Pruschke, K. Held, D. Vollhardt, and V. I. Anisimov, Phys. Rev. Lett. **93**, 156402 (2004).

[13] X. Y. Zhang, M. J. Rozenberg, and G. Kotliar, Phys. Rev. Lett. **70**, 1666 (1993).

[14] M. J. Rozenberg, G. Kotliar, H. Kajueter, G. A. Thomas, D. H. Rapkine, J. M. Honig, and P. Metcalf, Phys. Rev. Lett. **75**, 105 (1995).

[15] V. I. Anisimov, D. E. Kondakov, A. V. Kozhevnikov, I. A. Nekrasov, Z. V. Pchelkina, J. W. Allen, S.-K. Mo, H.-D. Kim, P. Metcalf, S. Suga, A. Sekiyama, G. Keller, I. Leonov, X. Ren, and D. Vollhardt, Phys. Rev. B **71**, 125119 (2005).

[16] I. A. Nekrasov, G. Keller, D. E. Kondakov, A. V. Kozhevnikov, T. Pruschke, K. Held, D. Vollhardt, and V. I. Anisimov, Phys. Rev. B **72**, 155106 (2005).

[17] T. Higuchi, S. Nozawa, T. Tsukamoto, H. Ishii, R. Eguchi, Y. Tezuka, S. Yamaguchi, K. Kanai, and S. Shin, Phys. Rev. B **66**, 153105 (2002).

[18] Y. Taguchi, Y. Tokura, T. Arima, and F. Inaba, Phys. Rev. B **48**, 511 (1993).

[19] Y. Tokura, Y. Taguchi, Y. Moritomo, K. Kumagai, T. Suzuki, and Y. Iye, Phys. Rev. B **48**, 14063 (1993).

[20] M. Tsubota, F. Iga, T. Takabatake, N. Kikugawa, T. Suzuki, I. Oguro, H. Kawanaka, and H. Bo, Physica B **281-282**, 622 (2000).

[21] M. Tsubota, F. Iga, T. Nakano, K. Uchihira, S. Kura, M. Takemura, Y. Bo, K. Umeo, T. Takabatake, E. Nishibori, M. Takata, M. Sakata, K. Kato, and Y. Ohishi, J. Phys. Soc. Jpn. **72**, 3182 (2003).

[22] M. Arita, Y. Takeda, Y. Okamura, H. Sato, K. Shimada, K. Mamiya, H. Namatame, M. Taniguchi, M. Tsubota, F. Iga, and T. Takabatake, Physica B **281-282**, 617 (1999).

[23] M. Arita, Y. Takeda, Y. Okamura, H. Sato, K. Shimada, K. Mamiya, H. Namatame, M. Taniguchi, M. Tsubota, F. Iga, and T. Takabatake, Jpn. J. Appl. Phys., Suppl. **38**, 206 (1999).

[24] K. Yokoyama, K. Nishihara, K. Mimura, Y. Hari, M. Taniguchi, Y. Ueda, and M. Fujisawa, Rev. Sci. Instrum. **64**, 87 (1993).

[25] Y. Ueda, K. Nishikawa, K. Mimura, Y. Hari, M. Taniguchi, and M. Fujisawa, Nucl. Instrum. Methods Phys. Res. A **330**, 140 (1993).

[26] H. Sato, T. Kotsugi, S. Senba, H. Namatame, and M. Taniguchi, J. Synchrotron Radiat. **5**, 772 (1998).

[27] We have tentatively attempted various normalization procedures using the intensities around some energy positions between 7 and 15 eV, and the intensities integrated between 10 and 17 eV and between −3 and 5 eV. The results shown below were independent of the procedures.

[28] The fluorescence peaks are weaker and broader than the main structures. Hence the peaks do not affect the results of the CFS spectra even if the peaks cross the energy position used for the normalization.

[29] K. E. Smith and V. E. Henrich, Phys. Rev. B **38**, 9571 (1988).

[30] T. Higuchi, T. Tsukamoto, S. Yamaguchi, Y. Tezuka, and S. Shin, Jpn. J. Appl. Phys., Part 2 **40**, L201 (2001).

[31] J. Barth, I. Chorkendorff, F. Gerken, C. Kunz, R. Nyholm, J. Schmidt-May, and G. Wendin, Phys. Rev. B **30**, 6251 (1984).

[32] S. Saha, T. P. Sinha, and A. Mookerjee, Eur. Phys. J. B **18**, 207 (2000).

[33] The structure in the Ca $3d$ partial DOS calculated for cubic perovskite-type structure appears around 3.5 eV, while the Ti $3d$ e_g states hybridized with the O $2p$ and Ca $3d$ states are observed as the broad structure between 3 and 8 eV in the off-resonance spectrum of $CaTiO_3$ with $GaFeO_3$-type distortion. The discrepancy could be attributed to an increase in Ca-O covalency due to $GaFeO_3$-type distortion in $CaTiO_3$.

[34] H. Fujitani and S. Asano, Phys. Rev. B **51**, 2098 (1995).

[35] M. Arita (unpublished).

[36] E. Pavarini, S. Biermann, A. Poteryaev, A. I. Lichtenstein, A. Georges, and O. K. Andersen, Phys. Rev. Lett. **92**, 176403 (2004).